

COMPARATIVE STUDY OF THE $\text{MeV}_2\text{O}_6\text{-MoO}_3\text{-Li}_2\text{O}$ PHASE DIAGRAMS

Jacek Ziólkowski and Krzysztof Mocała
Institute of Catalysis and Surface Chemistry
Polish Academy of Sciences, Kraków, Poland

ABSTRACT

Comparative study involves the following subsystems of $\text{MeO-Li}_2\text{O-V}_2\text{O}_5\text{-MoO}_3$: $\text{MnV}_2\text{O}_6\text{-MoO}_3$, $\text{MnV}_2\text{O}_6\text{-LiVMoO}_6\text{-MoO}_3$, $\text{CoV}_2\text{O}_6\text{-MoO}_3$, $\text{ZnV}_2\text{O}_6\text{-MoO}_3$ and $\text{ZnV}_2\text{O}_6\text{-LiVMoO}_6\text{-MoO}_3$. Solid solutions $\text{Me}_{1-x}\phi_x\text{V}_{2-2x}\text{Mo}_{2x}\text{O}_6$ or $\text{Me}_{1-x-y}\phi_x\text{Li}_y\text{V}_{2-2x-y}\text{Mo}_{2x+y}\text{O}_6$ (ϕ - cation vacancy at Me site) are located in these subsystems. Phase diagrams are determined with DTA and X-ray phase analysis. Some of them (Mn-containing) are natural subdiagrams of $\text{T-MeO-Li}_2\text{O-V}_2\text{O}_5\text{-MoO}_3$ (up to 760°C), the others represent only arbitrary subsystems.

EXPERIMENTAL

This study is based partly upon published (1 - 4) ($\text{MnV}_2\text{O}_6\text{-MoO}_3$, $\text{MnV}_2\text{O}_6\text{-LiVMoO}_6\text{-MoO}_3$, $\text{CoV}_2\text{O}_6\text{-MoO}_3$ systems) and partly upon unpublished data ($\text{ZnV}_2\text{O}_6\text{-MoO}_3$, $\text{ZnV}_2\text{O}_6\text{-LiVMoO}_6\text{-MoO}_3$). DTA curves were recorded with SETARAM M5 microanalyzer, in air, at a heating rate of $10^\circ/\text{min}$; Al_2O_3 preheated at 1500°C and Brazilian quartz were used as references. X-ray diffraction patterns were obtained with DRON-2 diffractometer using $\text{CuK}\alpha$ or $\text{CrK}\alpha$ radiation and an internal standard of Al. Magnetic susceptibility measurements and EPR were also used to verify the formulas of the studied solid solutions. Detail experimental procedure including preparation of samples and a brief summary of the literature data are given in the quoted papers (1 - 4).

RESULTS AND CONCLUSIONS

A number of bivalent metal vanadates MeV_2O_6 (Me = Mn, Co, Zn, Cu, Cd, Mg) crystallizes in the brannerite type structure. In this structure VO_6 octahedra, sharing three edges, form anionic sheets parallel to the (001) plane, and Me^{2+} ions, binding these sheets together, are located in octahedral interlayer positions (5, 6). Doping with MoO_3 results in formation of the solid solutions $\text{Me}_{1-x}\phi_x\text{V}_{2-2x}\text{Mo}_{2x}\text{O}_6$ (Me ϕ -type, Me = Mn, Co, Zn), in which Mo^{6+} ions are substituted at random for V^{5+} ions, and charge compensation is accomplished by ceration of an equivalent number of cationic vacancies ϕ , statistically distributed

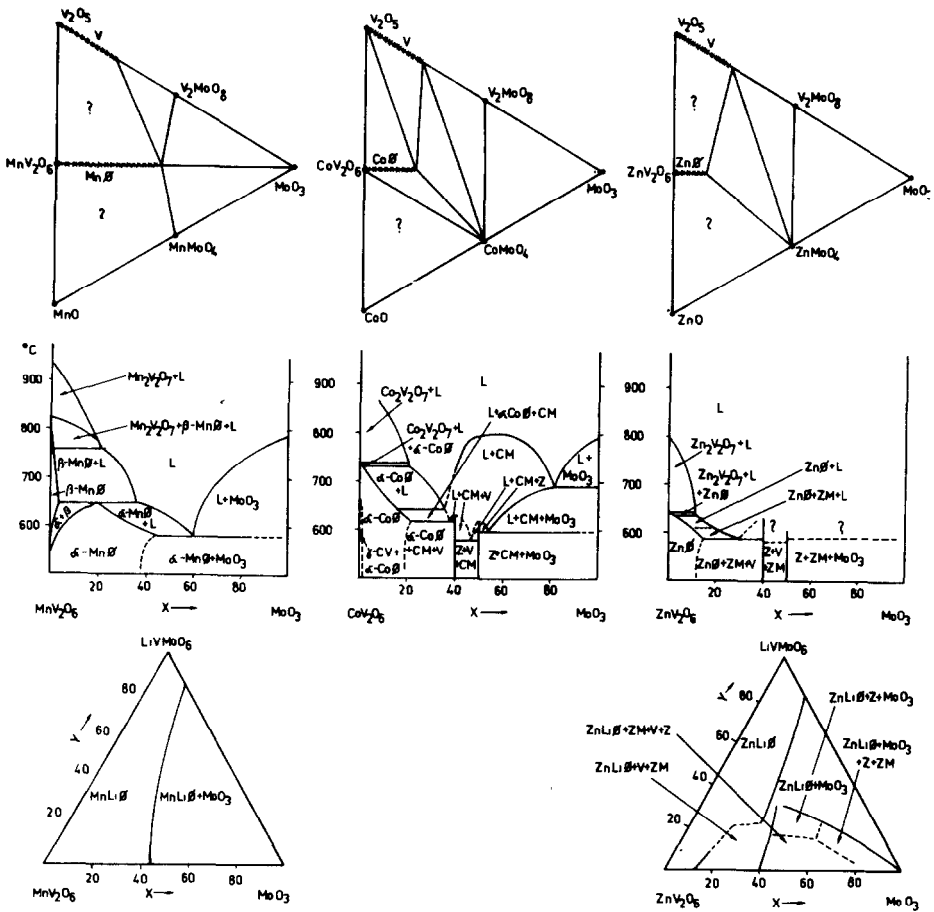


Fig. 1

Upper row: Division of the $\text{MeO}-\text{V}_2\text{O}_5-\text{MoO}_3$ systems into the natural subsystems (fields which have not been studied in detail are marked with question mark).

Middle row: $T-\text{MeV}_2\text{O}_6-\text{MoO}_3$ slices of the $T-\text{MeO}-\text{V}_2\text{O}_5-\text{MoO}_3$ diagrams.

Lower row: Subsolidus of the $\text{MeV}_2\text{O}_6-\text{LiVMeO}_6-\text{MoO}_3$ subsystems of the $\text{MeO}-\text{Li}_2\text{O}-\text{V}_2\text{O}_5-\text{MoO}_3$ system.

V = solid solution of MoO_3 in V_2O_5 , Z = V_2MoO_8 , CV = CoV_2O_6 , CM = CoMoO_4 , ZM = ZnMoO_4 , L = liquid, X = 100x, Y = 100 y.

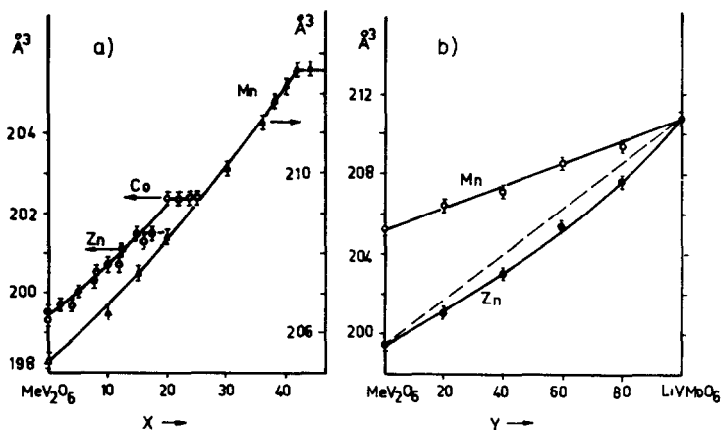
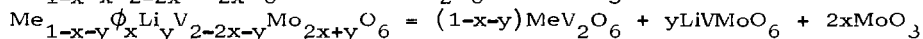
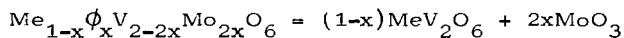


Fig. 2

Unit cell volume vs composition for MnO , CoO , ZnO (a) and for $MnLiO$ and $ZnLiO$, along the MeV_2O_6 - $LiVMoO_6$ arms of the MeV_2O_6 - $LiVMoO_6$ - MoO_3 triangles (b).

among the bivalent metal sites. An alternative way of charge compensation consists in incorporation of Li^+ ions into the Me sites: $Me_{1-x-y}O_x Li_y V_{2-2x-y} Mo_{2x+y} O_6$ ($MnLiO$ -type, $Me = Mn, Zn$). The abovementioned MeO and $MeLiO$ solid solutions belong to the ternary MeO - V_2O_5 - MoO_3 or quaternary MeO - Li_2O - V_2O_5 - MoO_3 systems, respectively. However, due to the stoichiometric limitations:



the composition of MeO and $MeLiO$ falls in fact within the pseudobinary MeV_2O_6 - MoO_3 or pseudoternary MeV_2O_6 - $LiVMoO_6$ - MoO_3 subsystems.

To define the range of stability of MeO and $MeLiO$ solid solutions in the T - x - y coordinates the phase diagrams of the abovementioned systems have been determined using DTA and X-ray phase analysis. The selected results are shown in Fig. 1.

In spite of high chemical analogies of the studied systems the determined phase diagrams are strongly differentiated in their shape. T - MnV_2O_6 - MoO_3 and T - MnV_2O_6 - $LiVMoO_6$ - MoO_3 diagrams have been found to be the natural subdiagrams of the respective ternary or quaternary systems up to 760 - 785°C. This means in particular, that in the subsolidus range two regions may be distinguished, in which either MeO

and $\text{Me}\phi_{\text{sat}} + \text{MoO}_3$ or $\text{MeLi}\phi$ and $\text{MeLi}\phi_{\text{sat}} + \text{MoO}_3$ are stable, respectively (saturated solutions are distinguished with index "sat"). Only above $760 - 785^\circ\text{C}$, due to the incongruent melting of MnV_2O_6 , $\text{Mn}_2\text{V}_2\text{O}_7$ and liquid appear in the system, the composition of which cannot be expressed on the chosen subdiagram scale, as the respective tie lines pierce the plane or the space of the subdiagrams. This is not so for $\text{T-CoV}_2\text{O}_6\text{-MoO}_3$ and $\text{T-ZnV}_2\text{O}_6\text{-MoO}_3$ subdiagrams, where above x_{sat} three ranges may be distinguished, in which $\text{Me}\phi_{\text{sat}} + \text{MeMoO}_4 + \text{V}_{\text{sat}}$, $\text{MeMoO}_4 + \text{V}_{\text{sat}} + \text{Z}$ and $\text{MeMoO}_4 + \text{Z} + \text{MoO}_3$ coexist (V = solid solution of MoO_3 in V_2O_5 , $\text{Z} = \text{V}_2\text{MoO}_8$), proving that we deal with arbitrary slices in the whole studied temperature range. Consequently $\text{ZnV}_2\text{O}_6\text{-LiVMoO}_6\text{-MoO}_3$ is a complicated arbitrary subsystem of $\text{ZnO-Li}_2\text{O-V}_2\text{O}_5\text{-MoO}_3$. The following fields have been identified in its sub-solidus: $\text{ZnLi}\phi$, $\text{ZnLi}\phi_{\text{sat}} + \text{MoO}_3$, $\text{ZnLi}\phi_{\text{sat}} + \text{MoO}_3 + \text{Z}$, $\text{ZnLi}\phi_{\text{sat}} + \text{MoO}_3 + \text{Z} + \text{ZM}$, $\text{ZnLi}\phi_{\text{sat}} + \text{V}_{\text{sat}} + \text{ZM}$, $\text{ZnLi}\phi_{\text{sat}} + \text{V}_{\text{sat}} + \text{ZM} + \text{Z}$ ($\text{ZM} = \text{ZnMoO}_4$).

Both, the location of the lines representing the composition of the $\text{MnLi}\phi_{\text{sat}}$ and $\text{ZnLi}\phi_{\text{sat}}$ solutions (Fig.1, lower row) and the changes of the unit cell volume with composition for the solutions lying along the $\text{MeV}_2\text{O}_6\text{-LiVMoO}_6$ arms of the $\text{MeV}_2\text{O}_6\text{-LiVMoO}_6\text{-MoO}_3$ triangles (Fig.2b) prove that $\text{MnLi}\phi$ is the perfect (or nearly) solid solution, while $\text{ZnLi}\phi$ shows marked negative deviations from the Raoult's (or Vegard's) law. Little negative deviations are also seen for $\text{Mn}\phi$, $\text{Co}\phi$ and $\text{Zn}\phi$ solid solutions (Fig. 2a).

REFERENCES

1. R.Kozłowski, J.Ziółkowski, K.Mocała and J.Haber, J. Solid State Chem., 35 (1980) 1, erratum 38 (1981) 138
2. J.Ziółkowski, R.Kozłowski, K.Mocała and J.Haber, J. Solid State Chem., 35 (1980) 297
3. J.Ziółkowski, K.Krupa and K.Mocała, J.Solid State Chem., 48 (1983) 376
4. K.Mocała, J.Ziółkowski and L.Dziembaj, J. Solid State Chem., in press
5. R.Ruh and A.D.Wadsley, Acta Crystallogr., 21 (1966) 974
6. H.N.Ng and C.Calvo, Canad. J.Chem., 50 (1972) 3619